

Synthetic Applications of Synergism using Catalytic Binuclear Elimination Reactions. Further Examples of Rhodium-Manganese and Rhodium-Rhenium-Catalyzed Hydroformylations

Chuanzhao Li,^{a,b} Li Chen,^b and Marc Garland^{a,b,*}

^a Department of Chemical and Biomolecular Engineering, National University of Singapore, Singapore 117576

^b Institute of Chemical and Engineering Sciences, A*STAR (Agency for Science, Technology and Research), 1 Pesek Road, Jurong Island, Singapore 627833

Fax: (+65)-6316-6185; e-mail: marc_garland@ices.a-star.edu.sg

Received: January 7, 2008; Published online: March 12, 2008

Abstract: Synergism has been previously observed in both rhodium-manganese- and rhodium-rhenium-catalyzed hydroformylation. Furthermore, detailed *in situ* spectroscopic investigations have conclusively shown that the phenomenological origin of this synergistic effect is catalytic binuclear elimination (*J. Am. Chem. Soc.* **2003**, *125*, 5540–5548; **2007**, *129*, 13327–13334). In the present contribution, further substrates are used in the hydroformylation reaction with both rhodium-manganese and rhodium-rhenium. *In situ* spectroscopic studies show that (i) significant rate enhancements occur in the mixed metal systems with the new substrates and (ii) the organometallics present in the active systems, and their con-

centration profiles are consistent with those present in the previously studied catalytic binuclear elimination reactions (CBER). It is therefore concluded that catalytic binuclear elimination is a rather general mechanism in mixed metal hydroformylations and is rather independent of the substrates used. Further discussion is given to mechanistic aspects, synthetic efficiency, and the possibility that such synergistic effects might be useful to other classes of organic syntheses.

Keywords: catalytic binuclear elimination; hydroformylation; rhodium; spectroscopy; synergism; synthetic efficiency

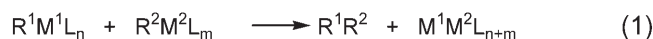
Introduction

Synergism is the term frequently used to describe the combined application of more than one metal, leading to regio-, chemo- and stereoselectivities and/or activities which differ significantly from a strictly additive effect.^[1,2] Accordingly, synergism holds considerable promise (perhaps greatly underutilized) as an approach for improving synthetic strategies and synthetic efficiency.

A number of phenomena have been proposed to explain synergistic observations in homogeneous catalysis. One of the most frequent has been cluster catalysis,^[3–5] i.e., the catalytic system consists of intermediates all having the same hetero-bimetallic or hetero-multimetallic nuclearity. Another explanation has been the simultaneous presence of intermediates with various nuclearities interacting in a complex manner. A well documented example involves the I/Ru/Ir-promoted carbonylation of methanol to acetic acid,^[6] where mononuclear ruthenium carbonyl, mononuclear iridium carbonyl and bimetallic ruthenium-iridium carbonyl complexes are simultaneously pres-

ent. In this system, ruthenium promotes the abstraction of iodine from an iridium compound, leading to coordinative unsaturation on iridium and then eventual elimination of acetic acid from an iridium compound. This is the synthetic basis for the well known, commercial and widely used Cativa process.

Another class of multiple-nuclearity catalytic systems, namely catalytic binuclear eliminations, has also been proposed as an origin of synergism.^[7] In such systems, binuclear elimination between two mononuclear intermediates leads to organic product formation and a dinuclear complex. Thus, these systems possess simultaneously both mononuclear and heterobinuclear complexes. Numerous examples exist in the literature for *stoichiometric* binuclear eliminations leading to organic products,^[8] and the catalytic version has been the focus of considerable work and debate.^[9–11] Eq. (1) shows a non-elementary step involving a hetero-bimetallic stoichiometric binuclear elimination, where R¹ and R² are ligands which eliminate to form the organic product R¹R², L are other li-



gands not involved in elimination, and M^1 and M^2 are different metallic elements.

Recently, the existence of the hetero-bimetallic catalytic binuclear elimination reaction (CBER) has been conclusively demonstrated in the hydroformylation reaction using rhodium-manganese and rhodium-rhenium mixed-metal systems.^[12] Detailed *in situ* FT-IR spectroscopic measurements showed the simultaneous presence of both mononuclear and dinuclear intermediates in the active systems. Detailed kinetic modelling demonstrated that the rate limiting and product forming steps were the attack of $\text{HM}(\text{CO})_5$ ($M = \text{Mn, Re}$) on $\text{RCORh}(\text{CO})_4$ ($\text{R} = \text{C}_5\text{H}_9, \text{CH}_2\text{CH}_2\text{C}(\text{CH}_3)_3$) to yield aldehyde. In the case of the rhodium-rhenium system, $\text{RhRe}(\text{CO})_9$ was spectroscopically observed and shown to activate molecular hydrogen at a very high rate. Perhaps most importantly, the catalytic binuclear elimination mechanism is synthetically much more efficient than the classic unicyclic mechanism which involves the hydrogenolysis $\text{RCORh}(\text{CO})_4$. In the CBER systems, $\text{HM}(\text{CO})_5$ is *ca.* 170–1200 times more reactive toward $\text{RCORh}(\text{CO})_4$ than molecular hydrogen. Scheme 1 shows a combined unicyclic and CBER mechanism for hydroformylation.

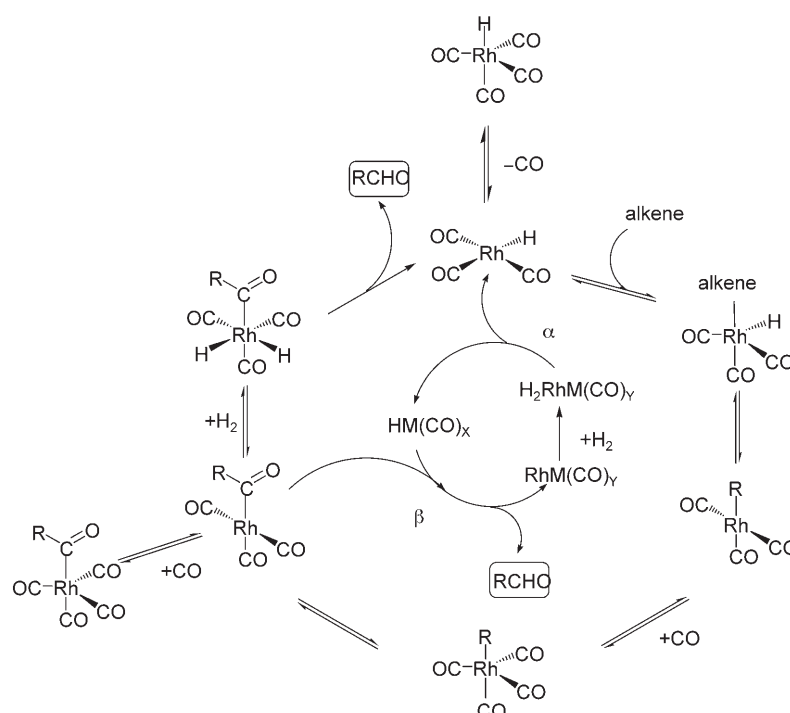
In the present contribution, the rhodium-manganese and rhodium-rhenium mixed-metal hydroformy-

lation systems are re-investigated using additional substrates. The immediate purpose is to demonstrate that hydroformylation CBER systems are not restricted to just a few substrates. The broader purpose is to highlight the synergistic effects and hence synthetic advantages of mixed-metal CBER. This might promote further consideration within the catalytic community of (1) other classes of organic syntheses which might be achieved using a similar approach and (2) other classes of organic syntheses which might be more rapidly or selectively achieved using a similar approach.

Results

Rhodium-Rhenium Systems

The organometallics $\text{Rh}_4(\text{CO})_{12}$ and $\text{HRe}(\text{CO})_5$ were used as precursors in this section. Separate hydroformylation experiments were conducted with the substrates 3,3-dimethylbut-1-ene, styrene, and methylene cyclohexane. *In situ* spectroscopic FT-IR measurements were conducted for each system, and the signals were analysed using the BTEM algorithm. The experimental and computational issues are presented in the Experimental Section.



Scheme 1. A combined unicyclic and CBER mechanism for mixed metal-catalyzed hydroformylation. The outer cycle consists of just mononuclear rhodium intermediates and represents the classic hydroformylation mechanism. In this scheme, CBER is made possible by (1) a step α representing the transformation of a dinuclear complex to mononuclear complexes and (2) a step β representing binuclear elimination.

Observable Species Present

The spectroscopic results using 3,3-dimethylbut-1-ene as substrate were selected to illustrate the methods used for detailed analysis. A total of 120 spectra were first subjected to singular value decomposition. The resulting right singular vectors (basis vectors for the observable components) are ordered according to their contribution to the total signal variance and some of these are shown in Figure 1. Localized signals with good signal-to-noise ratios were clearly observed in the first *ca.* 20 right singular vectors. In contrast, the right singular vectors from the 50th vector onwards consist of more-or-less randomly distributed white noise.

Since most of the useful signals associated with the observable components are present in the first *ca.* 20–25 right singular vectors, these were taken for further analysis using the BTEM algorithm. The resulting pure component spectral estimates are shown in Figure 2. The pure component spectra of the solvent and dissolved CO as well as the organic reactants 3,3-dimethylbut-1-ene and 4,4-dimethylpentanal were easily recovered. In addition, good spectral estimates for four observable organometallics were obtained, namely, $\text{Rh}_4(\text{CO})_{12}$, $\text{HRe}(\text{CO})_5$, $\text{RCORh}(\text{CO})_4$ ^[13] and $\text{RhRe}(\text{CO})_9$ ^[14]. All of these organometallic species were present at concentrations of 80 ppm or less. The last two species are non-isolatable complexes formed under reaction conditions.

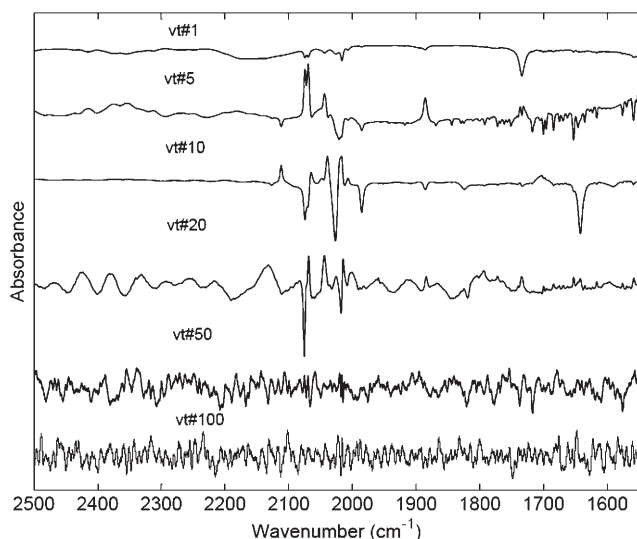


Figure 1. The right singular vectors from a singular value decomposition of the *in situ* FT-IR spectroscopic data from the Rh-Re catalyzed hydroformylation of 3,3-dimethylbut-1-ene.

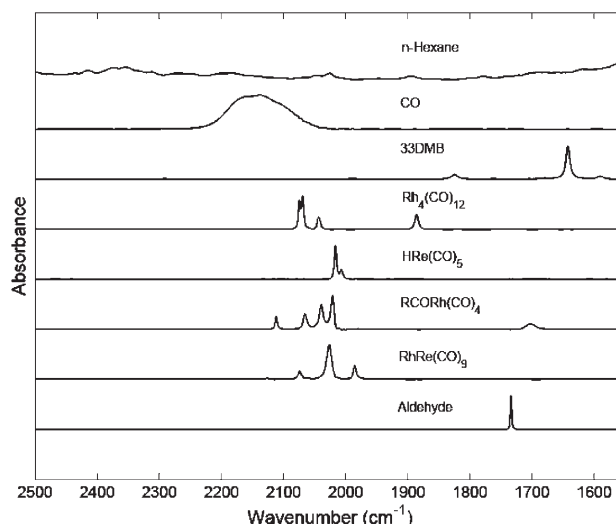


Figure 2. The BTEM recovered pure component spectra of the solute species from the Rh-Re-catalyzed hydroformylation of 3,3-dimethylbut-1-ene.

The Time-Dependent Concentrations Of Organometallics

The time-dependent concentrations of the reactive solutes were determined using an algebraic system identification algorithm (see Experimental Section for details). The time-dependent concentrations of all four observable organometallics were obtained and these are shown in Figure 3a. It is seen that the concentrations of the organometallic precursors $\text{Rh}_4(\text{CO})_{12}$ and $\text{HRe}(\text{CO})_5$ decrease and the intermediates $\text{RCORh}(\text{CO})_4$ and $\text{RhRe}(\text{CO})_9$ increase at initial reaction times. At *ca.* 80 min, the concentrations of all observable organometallics have reached a pseudo-steady state. It is noteworthy that the concentration profiles are quite smooth, even at the very low concentrations present. This is due in part to the high-quality *in situ* spectroscopic measurements but also due to the multivariate numerical methods used. The organometallics present in this active system, namely $\text{Rh}_4(\text{CO})_{12}$, $\text{HRe}(\text{CO})_5$, $\text{RCORh}(\text{CO})_4$ and $\text{RhRe}(\text{CO})_9$, are the same as those observed in the hydroformylation of cyclopentene which was modelled previously in considerable detail elsewhere.^[12d] For comparison purposes, the time-dependent concentrations for $\text{Rh}_4(\text{CO})_{12}$ and $\text{RCORh}(\text{CO})_4$ from a pure rhodium-catalyzed hydroformylation are also shown in Figure 3b. Comparison of Figure 3a and b shows that the presence of $\text{HRe}(\text{CO})_5$ accelerates the transformation of $\text{Rh}_4(\text{CO})_{12}$ to $\text{RCORh}(\text{CO})_4$. This phenomenon has been attributed to the attack of $\text{HRe}(\text{CO})_5$ on a transient species $\{\text{Rh}_4(\text{CO})_{14}\}$ and this has been modelled in detail elsewhere.^[12d]

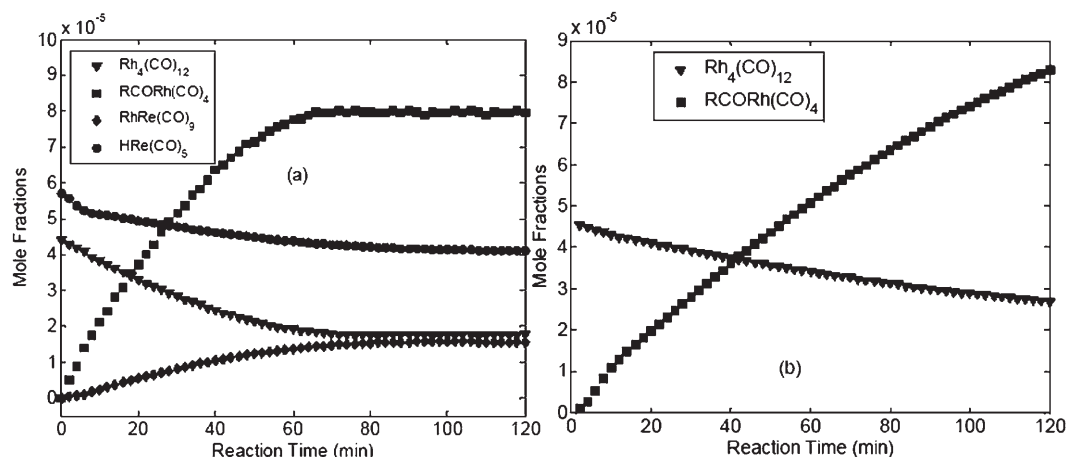


Figure 3. The time-dependent mole fractions of the organometallic solutes. (a) Initial reaction conditions were 12.0 mg $\text{Rh}_4(\text{CO})_{12}$, 4.5 μL $\text{HRe}(\text{CO})_5$. (b) Initial reaction conditions were 13.8 mg $\text{Rh}_4(\text{CO})_{12}$. Both reactions used 0.5 mL 3,3-dimethylbut-1-ene in 50 mL hexane with 2.0 MPa CO and 1.0 MPa H_2 at 298.0 K.

Observable Increase in Rate of Product Formation

The time-dependent concentrations of the organic product 4,4-dimethylpentanal from the rhodium-rhenium system are shown in Figure 4. In addition, and for comparison purposes, the time-dependent concentrations of 4,4-dimethylpentanal in a pure rhodium hydroformylation at comparable conditions are also shown in this figure. It is clearly seen that the rhodium-rhenium system is significantly more active than the pure-rhodium system. Specifically at 120 min the rates of hydroformylation were 1.2×10^{-4} mole frac-

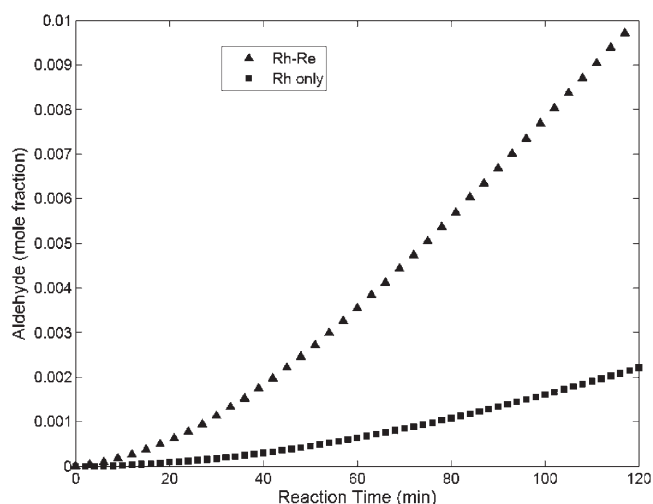


Figure 4. A comparison of the time-dependent mole fractions of the organic product 4,4-dimethylpentanal in a pure Rh-catalyzed hydroformylation and a Rh-Re-catalyzed hydroformylation. Initial reaction conditions for Rh-Re were 12.0 mg $\text{Rh}_4(\text{CO})_{12}$, 4.5 μL $\text{HRe}(\text{CO})_5$. Initial reaction conditions for Rh only were 13.8 mg $\text{Rh}_4(\text{CO})_{12}$. Both reactions used 0.5 mL 3,3-dimethylbut-1-ene in 50 mL hexane with 2.0 MPa CO and 1.0 MPa H_2 at 298.0 K.

tion/min (Rh-Re system) and 2.5×10^{-5} mole fraction/min (Rh system). This marked rate increase is analogous to that observed in the previously reported hydroformylation of cyclopentene.^[12d]

Remarks for Styrene and Methylene-Cyclohexane

BTEM analysis of the other two systems, using styrene and methylenecyclohexane as substrates, also resulted in the observation of $\text{Rh}_4(\text{CO})_{12}$, $\text{HRe}(\text{CO})_5$, $\text{RCORh}(\text{CO})_4$ and $\text{RhRe}(\text{CO})_9$ in the active mixed-metal systems. In addition, significant hydroformylation rate increases were observed for both systems. The corresponding concentrations of the total aldehyde products are shown in Figure 5 and Figure 6. Since styrene and methylenecyclohexane are less reactive than 3,3-dimethylbut-1-ene, slightly longer reaction times are shown.

Kinetic Modelling of Product Formation

In mixed rhodium-rhenium hydroformylation, there are two simultaneous mechanisms for product formation. Accordingly, there are two simultaneous product forming steps. These are (1) the hydrogenolysis of the rhodium intermediate $\text{RCORh}(\text{CO})_4$ and (2) the attack of $\text{HRe}(\text{CO})_5$ on $\text{RCORh}(\text{CO})_4$. Since the instantaneous concentrations of these organometallics as well as the organic product can be measured, the contributions of each mechanism to total product formation can be evaluated. Eq. (2) describes this total

$$r_{\text{Total}} = k_1[\text{RCORh}(\text{CO})_4][\text{H}_2][\text{CO}]^{-1} + k_2[\text{RCORh}(\text{CO})_4][\text{HRe}(\text{CO})_5][\text{CO}]^{-1.6} \quad (2)$$

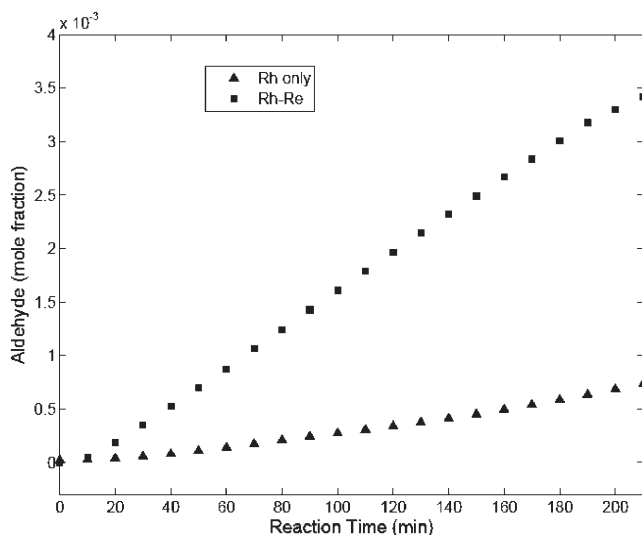


Figure 5. A comparison of the time-dependent mole fractions of the organic product phenylpropanal in a pure Rh-catalyzed hydroformylation and a Rh-Re-catalyzed hydroformylation. Initial reaction conditions for Rh-Re were 36.3 mg $\text{Rh}_4(\text{CO})_{12}$, 45 μL $\text{HRe}(\text{CO})_5$. Initial reaction conditions for Rh only were 91.2 mg $\text{Rh}_4(\text{CO})_{12}$. Both reactions used 25 mL styrene in 300 mL hexane with 5.0 MPa CO and 0.5 MPa H_2 at 308.0 K.

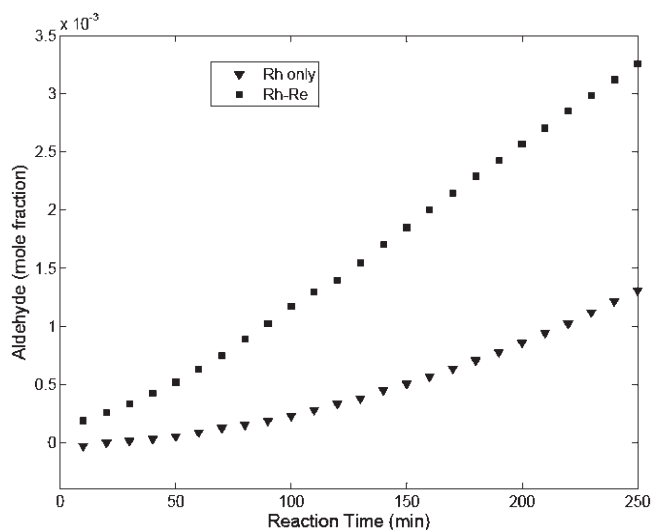


Figure 6. A comparison of the time-dependent mole fractions of the organic product 2-cyclohexylacetaldehyde in a pure Rh-catalyzed hydroformylation and a Rh-Re-catalyzed hydroformylation. Initial reaction conditions for Rh-Re were 40.3 mg $\text{Rh}_4(\text{CO})_{12}$, 20 μL $\text{HRe}(\text{CO})_5$. Initial reaction condition for Rh only was 52.3 mg $\text{Rh}_4(\text{CO})_{12}$. Both reactions used 2.1 mL methylenecyclohexane in 300 mL hexane with 2.0 MPa CO and 2.0 MPa H_2 at 289.7 K.

rate of formation for aldehydes where the reaction orders have been determined previously.^[12d] Finally, the total rate can be conveniently partitioned into

two parts, as shown in Eq. (3), to reflect the contributions from the unicyclic rhodium catalysis and the rhodium-rhenium CBER.

$$r_{\text{Total}} = \text{rate}_{\text{Rh}} + \text{rate}_{\text{Rh-Re CBER}} \quad (3)$$

The experimental runs using substrates 3,3-dimethylbut-1-ene, styrene, and methylenecyclohexane were analyzed using Eq. (2). The resulting coefficients k_1 and k_2 for the product forming steps are shown in Table 1. For comparison purposes, the results from pure rhodium hydroformylations are also included, as well as the previously reported result for the rhodium-rhenium hydroformylation of cyclopentene. Table 1 clearly shows that the k_1 values for acyl hydrogenolysis are consistent for each particular substrate (compare the value for the pure rhodium experiments and the mixed rhodium-rhenium experiments). In addition, it is clearly seen that the second term in Eq. (3), i.e., the attack of $\text{HRe}(\text{CO})_5$ on $\text{RCORh}(\text{CO})_4$ is the main contribution to product formation. When interpreting these results, it is instructive to recognize that the molar ratio of Re/H_2 in the liquid phase is very low, that is, on the order of 0.002 in all experiments. Therefore, it can be concluded that the CBER synthetic pathway utilizes rhodium far more effectively than the unicyclic synthetic pathway.

Rhodium-Manganese Systems

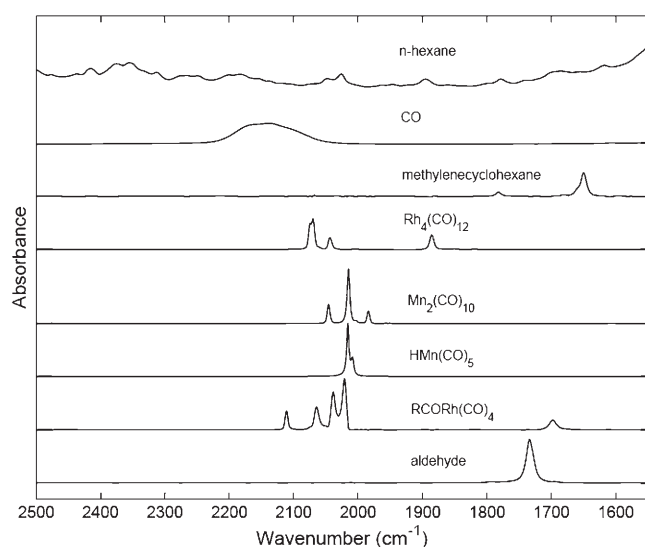
The organometallics $\text{Rh}_4(\text{CO})_{12}$ and a mixture of $\text{HMn}(\text{CO})_5/\text{Mn}_2(\text{CO})_{10}$ were used as precursors in this section (see Experimental Section). Separate hydroformylation experiments were conducted with the substrates styrene, and methylenecyclohexane. *In situ* spectroscopic FT-IR measurements were conducted for each system, and the signals were analyzed using the BTEM algorithm as demonstrated before.

Observable Species Present

The spectroscopic results using methylenecyclohexane were selected to illustrate the methods used for detailed analysis in this section. A total of 90 spectra were first subjected to singular value decomposition. Since most of the useful signals associated with the observable components are present in the first ca. 20–25 right singular vectors, these were taken for further analysis using the BTEM algorithm. The resulting pure component spectral estimates are shown in Figure 7. The pure component spectra of the solvent and dissolved CO as well as the organic reactants methylenecyclohexane and 2-cyclohexylacetaldehyde

Table 1. Kinetic parameters for Rh-Re hydroformylations.

Reaction Systems	Initial metal loading (mol ratio) $\text{HRe}(\text{CO})_5/\text{Rh}_4(\text{CO})_{12}$	k_1 (min^{-1})	k_2 (min^{-1})	$\text{rate}_{\text{Rh-Re CBER}}/\text{rate}_{\text{Rh}}$	T (K)	Remarks
3,3-Dimethylbut-1-ene with pure Rh	NA	0.48	NA	NA	298.0	This study
3,3-Dimethylbut-1-ene with Rh/Re	1.8	0.51	241	6.1	298.0	This study
Methylenecyclohexane with pure Rh	NA	0.05	NA	NA	289.7	This study
Methylenecyclohexane with Rh/Re	2.4	0.05	5.5	1.8	289.7	This study
Styrene with pure Rh	NA	3.4	NA	NA	308.0	This study
Styrene with Rh/Re	6.0	2.5	243	9.1	308.0	This study
Cyclopentene with Rh/Re	2.3	0.33	110	4.2	289.7	[12d]

**Figure 7.** The BTEM recovered pure component spectra of the solute species from the Rh-Mn-catalyzed hydroformylation of methylenecyclohexane.

were easily recovered. In addition, spectral estimates for four observable organometallics were obtained, namely, $\text{Rh}_4(\text{CO})_{12}$, $\text{HMn}(\text{CO})_5$, $\text{RCORh}(\text{CO})_4$ and $\text{Mn}_2(\text{CO})_{10}$.

The Time-Dependent Concentrations of Organometallics

The time-dependent concentrations of all four observable organometallics were obtained and are shown in Figure 8. It is seen that the concentrations of the organometallic precursors decrease and the intermediate $\text{RCORh}(\text{CO})_4$ increases at initial reaction times. Furthermore, it is seen that (i) the concentrations of all observable organometallics approach a pseudo-steady state very rapidly (more rapidly than the Rh-Re system) and (ii) the concentration of the limiting

precursor $\text{Rh}_4(\text{CO})_{12}$ approaches zero at long reaction times. Again, the concentration profiles are quite smooth, even at the very low concentrations present. The organometallics present in this active system, namely $\text{Rh}_4(\text{CO})_{12}$, $\text{HMn}(\text{CO})_5$, $\text{RCORh}(\text{CO})_4$ and $\text{Mn}_2(\text{CO})_{10}$ are the same as those observed in previous hydroformylations of 3,3-dimethylbut-1-ene and cyclopentene which were modelled in detail elsewhere.^[12a,b] For comparison purposes, the time-dependent concentrations for $\text{Rh}_4(\text{CO})_{12}$ and $\text{RCORh}(\text{CO})_4$ from a pure rhodium-catalyzed hydroformylation are also shown in Figure 8.

Observable Rate Increases

The time-dependent concentrations of the organic product 2-cyclohexylacetaldehyde from this rhodium-manganese system are shown in Figure 9. In addition, and for comparison purposes, the time-dependent concentrations of 2-cyclohexylacetaldehyde in a pure rhodium hydroformylation are also shown in this figure. It is clearly seen that the rhodium-manganese system is significantly more active than the pure rhodium system. Specifically at *ca.* 200 min the rates of hydroformylation were 2.6×10^{-5} mole fraction/min (Rh-Mn system) and 1.0×10^{-5} mole fraction/min (Rh system). This marked rate increase is analogous to that observed in the previous hydroformylations of 3,3-dimethylbut-1-ene and cyclopentene.^[12a,b]

Remarks for Styrene

BTEM analysis of the styrene system also resulted in the observation of $\text{Rh}_4(\text{CO})_{12}$, $\text{HMn}(\text{CO})_5$, $\text{RCORh}(\text{CO})_4$ and $\text{Mn}_2(\text{CO})_{10}$ in the active mixed-metal systems. In addition, significant hydroformylation rate increases were observed for this system. The corresponding concentrations of the total aldehyde products are shown in Figure 10.

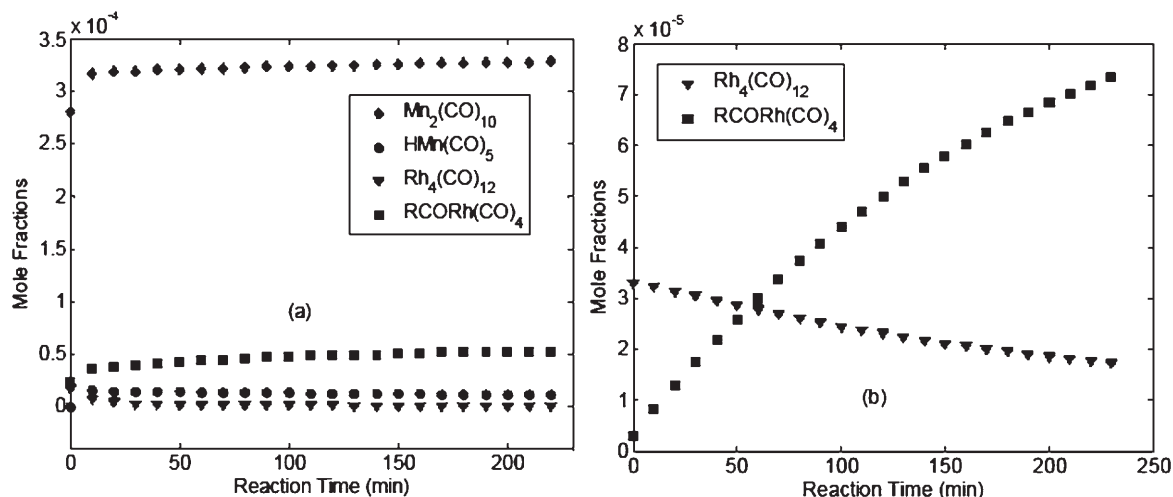


Figure 8. The time-dependent mole fractions of the organometallic solutes. (a) Initial reaction conditions were 18.1 mg Rh₄(CO)₁₂, and a mixture of HMn(CO)₅/Mn₂(CO)₁₀ obtained from 425.3 mg Mn₂(CO)₁₀; (b) Initial reaction conditions were 52.3 mg Rh₄(CO)₁₂, Both reactions used 2.1 mL methylenecyclohexane in 300 mL hexane with 2.0 MPa CO and 2.0 MPa H₂ at 289.7 K.

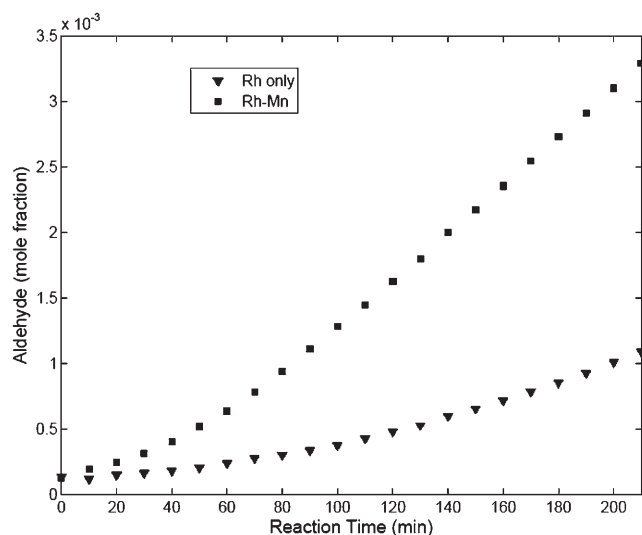


Figure 9. A comparison of the time-dependent mole fractions of the organic product 2-cyclohexylacetaldehyde in a pure Rh-catalyzed hydroformylation and an Rh-Mn-catalyzed hydroformylation. Initial reaction conditions for Rh-Mn were 18.1 mg Rh₄(CO)₁₂, and a mixture of HMn(CO)₅/Mn₂(CO)₁₀ obtained from 425.3 mg Mn₂(CO)₁₀; Initial reaction conditions for Rh only were 52.3 mg Rh₄(CO)₁₂, Both reactions used 2.1 mL methylenecyclohexane in 300 mL hexane with 2.0 MPa CO and 2.0 MPa H₂ at 289.7 K.

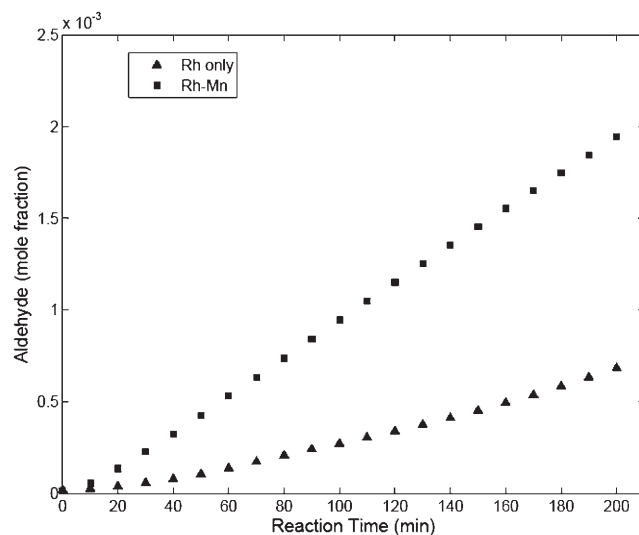


Figure 10. A comparison of the time-dependent mole fractions of the aldehyde in a pure Rh-catalyzed hydroformylation and an Rh-Mn-catalyzed hydroformylation. Initial reaction conditions for Rh-Mn were 91.5 mg Rh₄(CO)₁₂, and a mixture of HMn(CO)₅/Mn₂(CO)₁₀ obtained from 187.5 mg Mn₂(CO)₁₀; Initial reaction conditions for Rh only were 91.2 mg Rh₄(CO)₁₂, Both reactions used 25 mL styrene in 300 mL hexane with 5.0 MPa CO and 0.5 MPa H₂ at 308.0 K.

Kinetic Modelling of Product Formation

In mixed rhodium-manganese hydroformylation, there are two simultaneous mechanisms for product formation. Accordingly, there are two simultaneous product forming steps. These are (1) the hydrogenolysis of the rhodium intermediate RCORh(CO)₄ and

(2) the attack of HMn(CO)₅ on RCORh(CO)₄. Since the instantaneous concentrations of these organometallics as well as the organic product can be measured, the contributions of each mechanism to total product formation can be evaluated. Eq. (4) describes this total rate of formation for aldehydes where the reaction orders have been determined previously.^[12a,b] Fi-

Table 2. Kinetic parameters for Rh-Mn hydroformylations.

Reaction Systems	Initial metal loading (mol ratio) HMn(CO) ₅ /Rh ₄ (CO) ₁₂	k ₁ (min ⁻¹)	k ₂ (min ⁻¹)	rate _{Rh-Mn CBER} /rate _{Rh}	T (K)	Remarks
Methylenecyclohexane with pure Rh	NA	0.05	NA	NA	289.7	This study
Methylenecyclohexane with Rh/Mn	0.7	0.04	26	1.3	289.7	This study
Styrene with pure Rh	NA	3.4	NA	NA	308.0	This study
Styrene with Rh/Mn	0.2	3.4	192	1.2	308.0	This study
3,3-Dimethylbut-1-ene with Rh/Mn	0.4	0.45	44.5	1.3	298.0	[12a]
Cyclopentene with Rh/Mn	0.5	0.31	37	1.1	289.7	[12b]

$$r_{\text{Total}} = k_1[\text{RCORh}(\text{CO})_4][\text{H}_2][\text{CO}]^{-1} + k_2[\text{RCORh}(\text{CO})_4][\text{HMn}(\text{CO})_5][\text{CO}]^{-1.5} \quad (4)$$

nally, the total rate can be conveniently partitioned into two parts, as shown in Eq. (5), to reflect the con-

$$r_{\text{Total}} = \text{rate}_{\text{Rh}} + \text{rate}_{\text{Rh-Mn CBER}} \quad (3)$$

tribution from the unicyclic rhodium catalysis and the rhodium-manganese CBER.

The experimental runs using substrates methylenecyclohexane and styrene were analysed using Eq. (4). The resulting coefficients k_1 and k_2 for the product forming steps are shown in Table 2. For comparison purposes, the results from pure rhodium hydroformylations are also included, as well as the previously reported result for the rhodium-manganese hydroformylation of 3,3-dimethylbut-1-ene and cyclopentene. Table 2 clearly shows that the k_1 values for acyl hydrogenolysis are consistent for each particular substrate between the pure rhodium experiments and the mixed rhodium-manganese experiments. In addition, it is clearly seen that the second term in Eq. (5), that is, the attack of HMn(CO)₅ on RCORh(CO)₄ is the main contribution to product formation. Again, when interpreting these results, it is instructive to recognize that the molar ratio of HMn(CO)₅/H₂ in the liquid phase is on the order of 0.005 in all experiments.

Discussion

Rh-Re

The *in situ* spectroscopic results in the present mixed-metal rhodium-rhenium hydroformylations of 3,3-dimethylbut-1-ene, methylenecyclohexane and styrene showed that the active systems contain the observable organometallics Rh₄(CO)₁₂, HRe(CO)₅, RCORh(CO)₄ and RhRe(CO)₉. This observation, as well as the associated concentration profiles, is consistent with the previous mixed-metal rhodium-rhenium

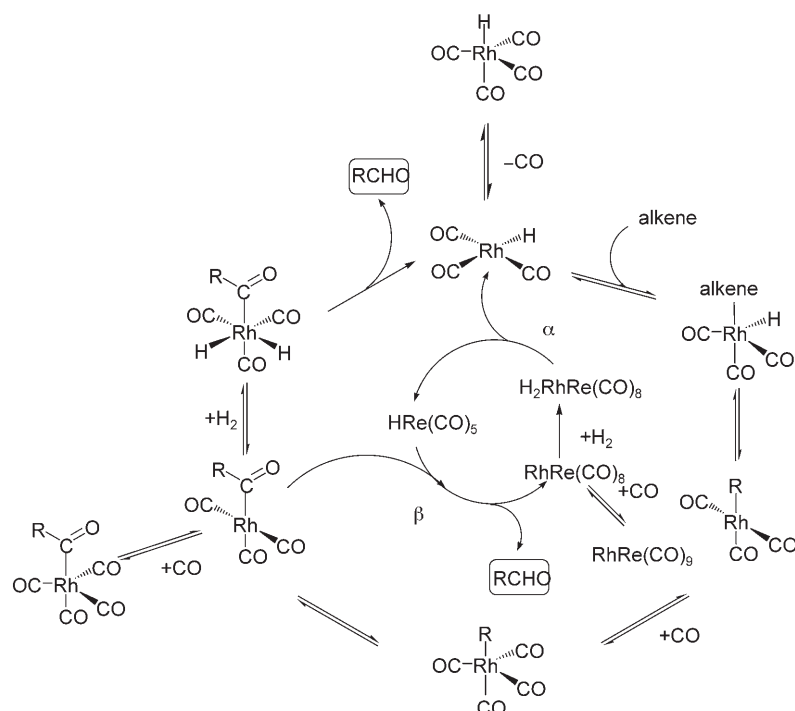
hydroformylation of cyclopentene. In addition, a significant synergistic rate increase was measured for all the present hydroformylations in the presence of Rh-Re as compared to just Rh. This too is consistent with the previous measurements of the mixed-metal rhodium-rhenium hydroformylation of cyclopentene. Simple regressions of the present total hydroformylation rates *versus* the time-dependent concentrations provided reasonable kinetic parameters. Taken together, these results support the conclusion that the present systems consist of two simultaneous catalytic systems (1) a classic unicyclic rhodium catalytic cycle consisting of only mononuclear intermediates and (2) a mixed metal rhodium-rhenium catalytic binuclear elimination. The interconnected mechanisms of the Rh-Re system are shown in Scheme 2.

Rh-Mn

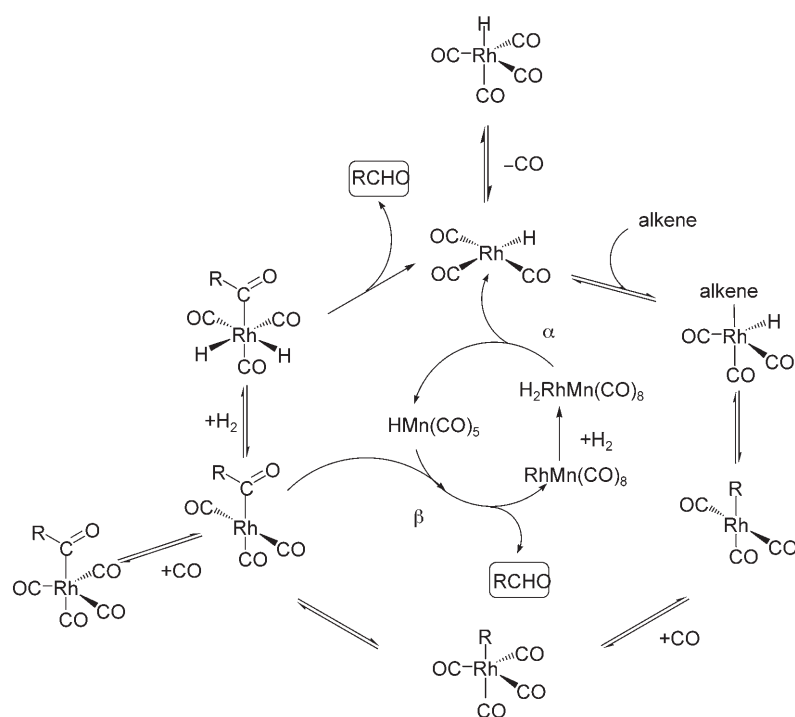
An analogous situation holds for the present mixed-metal rhodium-manganese [Rh₄(CO)₁₂ and HMn(CO)₅/Mn₂(CO)₁₀] hydroformylations of methylenecyclohexane and styrene. Indeed, the present hydroformylations behave very similarly to the previous rhodium-manganese hydroformylations of 3,3-dimethylbut-1-ene and cyclopentene. The expected organometallic species were observed in the active systems and their concentration profiles were similar, the expected rate increases were measured and regression of the results provided reasonable kinetic parameters. Accordingly, it is concluded that the present systems consist of two simultaneous catalytic systems (1) a classic unicyclic rhodium catalytic cycle consisting of only mononuclear intermediates and (2) a mixed metal rhodium-manganese catalytic binuclear elimination. The interconnected mechanisms of the Rh-Mn systems are shown in Scheme 3.

Implications for Organic Synthesis

The present study shows that synergistic CBER systems consisting of Rh-Re and Rh-Mn are not limited



Scheme 2. A combined unicyclic and CBER mechanism for Rh-Re-catalyzed hydroformylation. The outer cycle consists of just mononuclear rhodium intermediates and represents the classic hydroformylation mechanism.



Scheme 3. A combined unicyclic and CBER mechanism for Rh-Mn-catalyzed hydroformylation. The outer cycle consists of just mononuclear rhodium intermediates and represents the classic hydroformylation mechanism.

to just a few selected substrates. Therefore, Rh-Re and Rh-Mn CBER systems clearly have broader synthetic potential for hydroformylations.

The increased rates observed in these CBER type reactions provide a number of additional opportunities. These include (1) the possibility of dramatically

increasing rate using a cheaper base metal (or decreasing the loading of the precious metal), and (2) the possibility of dramatic process intensification.^[15] The latter issue arises from the bi-linear kinetics in metal loadings, and hence, the opportunities to decrease the volumes of reaction vessels (assuming that other mass-transfer effects, particularly gas-liquid mass transfer, do not interfere).

Opportunities probably exist for the development of new CBER type synthetic strategies for other types of reactions. This might include the identification of (1) other classes of organic syntheses which might be achieved using a similar approach and (2) other classes of organic syntheses which might be more rapidly or selectively achieved using a similar approach. Since one or both metals can be potentially modified in a CBER type catalytic system, a very broad range of possibilities are available to the experimentalist for fine-tuning synthetic aspects.

Conclusions

Additional mixed-metal Rh-Re and Rh-Mn hydroformylation systems have been investigated. *In situ* spectroscopy during these hydroformylation, together with kinetic modelling of product formation, indicate that these systems consist of two simultaneous mechanisms, namely, (1) a classic unicyclic rhodium catalytic cycle consisting of only mononuclear intermediates and (2) a mixed metal catalytic binuclear elimination. These results indicate the broader applicability of mixed-metal Rh-Re and Rh-Mn catalysis for hydroformylation, and suggest that CBER type synthetic strategies might be applicable to other classes of organic syntheses.

Experimental Section

General Information

All solutions preparations and transfers were carried out under purified argon (99.9995%, Saxol, Singapore) atmosphere using standard Schlenk techniques.^[16] The argon was further purified before use by passing it through a de-oxy and zeolite column. Purified carbon monoxide (Research grade, 99.7%, Saxol, Singapore) and purified hydrogen (99.9995%, Saxol, Singapore) were also further purified through de-oxy and zeolite columns before they were used in the hydroformylation experiments.

All precursors $\text{Rh}_4(\text{CO})_{12}$ (98%), $\text{Mn}_2(\text{CO})_{10}$ (98%) and $\text{HRe}(\text{CO})_5$ (99%) were purchased from Strem Chemicals (Newport, MA, USA) and were used as obtained. $\text{MnH}(\text{CO})_5$ was prepared using a modification^[12b] of a known literature preparation.^[17] This resulted in a mixture of $\text{Mn}_2(\text{CO})_{10}$ and $\text{MnH}(\text{CO})_5$ in *n*-hexane. The detailed procedure can be found in ref.^[12b] All alkenes, 3,3-dimethylbut-1-ene (99%), methylenecyclohexane (98%) and styrene

(99%) were purchased from Fluka. Styrene was distilled with CaH_2 under argon before use and the other two alkenes were used as obtained. The Puriss quality *n*-hexane (99.6%, Fluka AG) was distilled from sodium-potassium under argon for *ca.* 5 h to remove the trace water and oxygen.

Apparatus

The *in situ* kinetic studies were performed in two kinds of high-pressure FT-IR set-ups. For the hydroformylations performed in 300 mL of *n*-hexane, a 1.5-L stainless steel (SS316) autoclave ($P_{\text{max}}=22.5$ MPa, Buchi-Uster, Switzerland) connected with a high pressure infrared cell was used. The system is the same as that has been used for numerous rhodium hydroformylations by this group.^[18] The autoclave was equipped with a packed magnetic stirrer with six-bladed turbines in both the gas and liquid phases (autoclave Engineers, Erie PA) and has a mantle for heating/cooling. The liquid-phase reaction mixtures were circulated from the autoclave to and from the high pressure IR cell with a high pressure membrane pump (Model DMK 30, Orlita AG, Geissen Germany). A polyscience cryostat Model 9505 is used to keep the entire system isothermal ($\Delta t \leq 0.5$ °C) for the range 289–308 K. The high-pressure infrared cell was situated in a Perkin-Elmer Spectrum 2000 FT-IR spectrometer with spectral resolution 4 cm^{-1} and intervals 0.2 cm^{-1} for the range 1000–2500 cm^{-1} . The detailed experimental scheme can be found in ref.^[18d]

For the hydroformylations performed in 50 mL of *n*-hexane, an in-house designed 100-mL high pressure SS316 reactor was used, which was connected with an *in situ* injection block, and a high pressure magnetically driven gear pump (Model GAH-X2, Micro pump, USA). The high-pressure infrared cell was situated in a Bruker Vertex-70 FT-IR spectrometer and the spectral resolution was 2 cm^{-1} with an interval of 0.12 cm^{-1} for the range 1000–2500 cm^{-1} . A detailed description of the reactor, pump and injection block can be found elsewhere.^[19]

The high-pressure infrared cell was constructed at ETH Zurich using SS316 steel and could be heated and cooled. The CaF_2 single crystal window (Korth Monokristalle, Kiel Germany) has dimensions of 40 mm diameter by 15 mm thickness. Two sets of Viton and silicone gaskets provide the necessary sealing, and Teflon spacers are used between the windows.

In Situ Spectroscopic and Kinetic Studies

For the experiments carried out in the 1.5-L reactor, *n*-hexane was transferred under argon to the autoclave. The total system pressure was raised to the set CO partial pressure, and the stirrer and high-pressure membrane pump were started. Alkene solutions dissolved in 50 mL of *n*-hexane were prepared, transferred to the high-pressure reservoir under argon, pressurized with CO and then added to the autoclave. After equilibration, $\text{Rh}_4(\text{CO})_{12}$ dissolved in 50 mL of *n*-hexane and a solution of $\text{Mn}_2(\text{CO})_{10}/\text{HMn}(\text{CO})_5$ or $\text{HRe}(\text{CO})_5$ in *n*-hexane were prepared, transferred to the high-pressure reservoir under argon, pressurized with CO and then added to the autoclave. After equilibration, hydrogen was then added to initiate the syntheses.

Table 3. Experimental design.

Experiment	<i>n</i> -Hexane [mL]	Second Metal	CO [MPa]	H ₂ [MPa]	Alkene [mL]	Rh ₄ (CO) ₁₂ [mg]	Temp. [K]
3,3-Dimethylbut-1-ene with Rh	50	NA	2.0	1.0	0.5	13.8	298.0
3,3-Dimethylbut-1-ene with Rh/Re	50	HRe(CO) ₅ [4.5 μL]	2.0	1.0	0.5	12.0	298.0
Methylenecyclohexane with Rh	300	NA	2.0	2.0	2.1	52.3	289.7
Methylenecyclohexane with Rh/Re	300	HRe(CO) ₅ [20.0 μL]	2.0	2.0	2.1	40.3	289.7
Methylenecyclohexane with Rh/Mn	300	Mn ₂ (CO) ₁₀ [425.3 mg]	2.0	2.0	2.1	18.1	289.7
Styrene with Rh	300	NA	5.0	0.5	25.0	91.2	308.0
Styrene with Rh/Re	300	HRe(CO) ₅ [45.0 μL]	5.0	0.5	25.0	36.3	308.0
Styrene with Rh/Mn	300	Mn ₂ (CO) ₁₀ [187.5 mg]	5.0	0.5	25.0	91.5	308.0

For the hydroformylations performed in 50 mL of *n*-hexane, Rh₄(CO)₁₂ was dissolved in 50 mL of *n*-hexane and transferred under argon to the reactor. The system was pressurized with CO, the stirrer and high-pressure gear pump were started. Alkenes and HRe(CO) were injected through the injection valves and the reaction was initiated by adding H₂. The experimental design is listed in Table 3.

Conversions and Selectivities

In this study, initial rate data are emphasized. Thus conversions of substrates ranged from only *ca.* 10% (for some pure rhodium systems) to *ca.* 50% (for some mixed metal systems). Due to the rather low substrate loadings and due to these low conversions, the partial pressures of the gaseous reactants, namely H₂ and CO typically varied less than 10% in any run.

Some selectivity issues arise with the use of the alkenes 3,3-dimethylbut-1-ene, methylenecyclohexane and styrene. Although hydrogenation in unmodified rhodium-catalyzed hydroformylation at these low temperatures is virtually undetectable, regio-isomers of the resulting aldehydes are formed. Previous studies have shown that the linear to branched ratios were typically (i) greater than 95:5 when 3,3-dimethylbut-1-ene was used as the substrate,^[18a] (ii) greater than 95:5 when methylenecyclohexane was used as the substrate,^[18b] and (iii) *ca.* 85:15 when styrene was used as the substrate at 308 K.^[18d] Accordingly, in this study, products will be reported as 4,4-dimethylpentanal, 2-cyclohexylacetaldehyde, and lump-sum mixture of 2-phenylpropanal and 3-phenylpropanal.

Mass Transfer Issues

Both experimental systems have been characterized previously with respect to gas-liquid mass transfer and the overall mass transfer coefficients were obtained as 0.1 s⁻¹ for H₂ and 0.6 s⁻¹ for CO (1.5-L reactor, 200 rpm), and *ca.* 0.03 s⁻¹ for H₂ (25-mL reactor, 600 rpm, the present 100-mL reactor is geometrically similar to the 25-mL reactor).^[18,19] The max-

imum rate of hydroformylation observed in the 1.5-L reactor was *ca.* 6 × 10⁻⁷ mole/s and the maximum rate of hydroformylation observed in the 100-mL reactor was *ca.* 8 × 10⁻⁷ mole/s. Calculations confirm that all reactions performed in this study belong to the Hatta Category H, that is, infinitely slow reaction compared to gas-liquid mass transfer. Accordingly, the presently reported rates represent the intrinsic reaction kinetics and not mass-transfer controlled kinetics. Further details of such mass transfer considerations can be found elsewhere.^[20]

Spectroscopy Issues

The spectra from each experimental run were consolidated and analyzed with the spectral reconstruction algorithm band-target entropy minimization (BTEM) in order to recover the pure component spectra present. BTEM has been successfully used to analyze data from numerous homogeneously catalyzed reactions.^[12,21] Details of this algorithm can be found elsewhere.^[22] A review of this approach and its application to homogeneous catalysis can be found elsewhere.^[23]

After BTEM analysis, to obtain the pure component spectra and to enumerate the number of observable species present, further calculations were performed. These include (1) renormalization of the data in order to account for changes in path length of the high pressure cell as well as changes in the reaction volume^[24] as well as (2) further algebraic manipulations to obtain internal calibrations for all species present and all the instantaneous reagent concentrations.^[25] Mole fractions are used throughout this study.

Evaluation of Reaction Rates

A central difference scheme was used to evaluate all the observable reaction rates from the time-dependent concentration data. This approach has been shown to provide reliable reaction rates as well as estimates of turn-over-frequencies.^[26]

Acknowledgements

Part of this work was supported by the Science and Engineering Research Council of A*STAR (Agency for Science, Technology and Research), Singapore.

References

- [1] J. R. Kosak, *Chem. Ind.* **1996**, 68, 31–41.
- [2] G. Jenner, *J. Organomet. Chem.* **1988**, 346, 237–251.
- [3] a) E. L. Muetterties, *Bull. Soc. Chim. Belg.* **1975**, 84, 959–986; b) R. Ugo, *Catal. Rev. Sci. Eng.* **1975**, 11, 225–297; c) J. Lewis, B. F. G. Johnson, *Pure Appl. Chem.* **1975**, 44, 43–79; d) E. L. Muetterties, *Science* **1977**, 196, 839–848.
- [4] a) L. N. Lewis, *Chem. Rev.* **1993**, 93, 2693–2730; b) G. Suss-Fink, G. Meister, *Adv. Organomet. Chem.* **1993**, 35, 41–134.
- [5] R. D. Adams, F. A. Cotton, (Eds.), *Catalysis by di- and polynuclear metal cluster complexes*, Wiley, New York, **1998**.
- [6] a) G. J. Sunley, D. J. Watson, *Catal. Today* **2000**, 58, 293–307; b) R. Whyman, A. P. Wright, J. A. Iggo, B. T. Heaton, *J. Chem. Soc. Dalton Trans.* **2002**, 771–777; c) A. P. Wright, R. Whyman, R. J. Watt, G. E. Morris J. A. Iggo, B. T. Heaton, in: *13th International Symposium on Homogeneous Catalysis* (Book of Abstracts), Tarragona, Spain, **2002**, 245.
- [7] a) D. S. Breslow, R. F. Heck, *Chem. & Ind.* **1960**, 467; b) R. F. Heck, D. S. Breslow, *J. Am. Chem. Soc.* **1961**, 83, 4023–4027.
- [8] a) I. Kovacs, F. Ungvary, L. Marko, *Organometallics* **1986**, 5, 209–215; b) J. R. Norton, *Acc. Chem. Res.* **1979**, 12, 139–145; c) M. Christina, F. G. A. Stone, *Inorg. Chem.* **1972**, 11, 102–107; d) P. Renaut, G. Tainturier, B. Gautheron, *J. Organomet. Chem.* **1978**, 150, C9–C10; e) B. Martin, D. K. Warner, J. R. Norton, *J. Am. Chem. Soc.* **1986**, 108, 33–39; f) R. J. Hoxmeier, J. R. Blickensderfer, H. D. Kaez, *Inorg. Chem.* **1979**, 18, 3453–3461; g) I. Kovacs, C. D. Hoff, F. Ungvary, L. Marko, *Organometallics* **1985**, 4, 1347–1350.
- [9] a) K. H. von Brandes, H. B. Jonassen, *Z. Anorg. Allg. Chem.* **1966**, 343, 215–219; b) F. Ungvary, L. Marko, *J. Organomet. Chem.* **1969**, 20, 205–209; c) B. H. Byers, T. L. Brown, *J. Am. Chem. Soc.* **1977**, 99, 2528–2532; d) F. Ungvary, L. Marko, *Organometallics* **1983**, 2, 1608–1612; e) C. Hoff, F. Ungvary, R. B. King, L. Marko, *J. Am. Chem. Soc.* **1985**, 107, 666–671; f) J. R. Norton, W. Carter, J. Kelland, S. Okrasinski, *Advances in Chemistry Series*, **1978**, 167, 170–180; g) R. T. Edidin, K. Hennessy, A. Moody, S. Okrasinski, J. R. Norton, *New J. Chem.* **1988**, 12, 475–477; h) M. J. Nappa, R. Santi, S. Diefenbach, J. Halpern, *J. Am. Chem. Soc.* **1982**, 104, 619–621; i) M. J. Nappa, R. Santi, J. Halpern, *Organometallics* **1985**, 4, 34–41; j) C. K. Brown, D. Geoglou, G. Wilkinson, *J. Chem. Soc. A* **1971**, 3120–3127; k) J. Schwartz, J. Cannon, *J. Am. Chem. Soc.* **1974**, 96, 4721; l) J. C. Barborak, K. Cann, *Organometallics*, **1982**, 1, 1726–1728.
- [10] a) W. D. Jones, R. G. Bergman, *J. Am. Chem. Soc.* **1979**, 101, 5447–5449; b) W. D. Jones, J. Huggins, R. G. Bergman, *J. Am. Chem. Soc.* **1981**, 103, 4415–4423; c) J. P. Collman, J. Belmont, J. Brauman, *J. Am. Chem. Soc.* **1983**, 105, 7288–7794; d) I. P. Beletskaya, A. Z. Voskoboinikov, G. K. Magomedov, *Metalloorg. Khim.* **1989**, 2, 810–813; e) I. P. Beletskaya, G. K. Magomedov, A. Z. Voskoboinikov, *J. Organomet. Chem.* **1990**, 385, 289–295.
- [11] J. P. Collman, L. S. Hegedus, J. R. Norton, R. G. Finke, *Principles and Applications of Organotransition Metal Chemistry*, University Science Books, Mill Valley, **1987**.
- [12] a) C. Li, E. Widjaja, M. Garland, *J. Am. Chem. Soc.* **2003**, 125, 5540–5548; b) C. Li, E. Widjaja, M. Garland, *Organometallics* **2004**, 23, 4131–4138; c) G. Liu, C. Li, L. Guo, M. Garland, *J. Catal.* **2006**, 237, 67–78; d) C. Li, L. Chen, M. Garland, *J. Am. Chem. Soc.* **2007**, 129, 13327–13334.
- [13] M. Garland, G. Bor, *Inorg. Chem.* **1989**, 28, 410–413.
- [14] C. Li, L. Guo, M. Garland, *Organometallics* **2004**, 23, 5275–5279.
- [15] C. Ramshaw, *Green Chem.* **1999**, 1, G15–G17.
- [16] D. F. Shriver, M. A. Drezdson, *The Manipulation of Air-Sensitive Compounds*, Wiley, New York, **1986**.
- [17] B. H. Byers, T. L. Brown, *J. Am. Chem. Soc.* **1977**, 99, 2527–2532.
- [18] a) M. Garland, P. Pino, *Organometallics* **1990**, 10, 1693–1704; b) G. Liu, R. Volken, M. Garland, *Organometallics* **1999**, 18, 3429–3436; c) J. Feng, M. Garland, *Organometallics* **1999**, 18, 417–427; d) J. Feng, M. Garland, *Organometallics* **1999**, 18, 1542–1546.
- [19] F. Gao, K. Ng, C. Li, K. Krummel, A. Allian, M. Garland, *J. Catal.* **2006**, 237, 49–57.
- [20] M. Garland, *Transport Effects in Homogeneous Catalysis*, in: *Encyclopedia of Catalysis*, (Ed.: I. T. Horvath), Wiley, New York, **2002**.
- [21] C. Li, E. Widjaja, W. Chew, M. Garland, *Angew. Chem.* **2002**, 114, 3939–3943; *Angew. Chem. Int. Ed.* **2002**, 41, 3785–3789.
- [22] a) W. Chew, E. Widjaja, M. Garland, *Organometallics* **2002**, 21, 1882–1990; b) E. Widjaja, C. Li, M. Garland, *Organometallics* **2002**, 21, 1991–1997.
- [23] M. Garland, in: *Mechanisms in Homogeneous Catalysis: A Spectroscopic Approach*, (Ed.: B. Heaton), Wiley, Weinheim, **2005**, pp 151–193.
- [24] W. Chew, E. Widjaja, M. Garland, *Applied Spectroscopy*, **2007**, 61, 734–746.
- [25] E. Widjaja, C. Li, M. Garland, *J. Catal.* **2004**, 223, 278–289.
- [26] R. Shirt, M. Garland, D. W. T. Rippin, *Anal. Chim. Acta* **1998**, 374, 67–91.